Received: 3 April 2023 | Revised: 6 March 2024 | Accepted: 13 March 2024

DOI: 10.1002/mp.17085

RESEARCH ARTICLE

MEDICAL PHYSICS

Automated determination of the ion-recombination correction factor (k_{sat}) in ultra-high dose rate electron radiation therapy

Michaël Claessens[1,2] | **Verdi Vanreusel**[1,2,3] | **Alessia Gasparini**[1,2] | **Luana de Freitas Nascimento**[3] | **Burak Yalvec**[4] | **Brigitte Reniers**[4] | **Dirk Verellen**[1,2]

[1]Department of Radiation Oncology, Iridium Netwerk, Wilrijk, Antwerp, Belgium

[2]Centre for Oncological Research (CORE), Integrated Personalized and Precision Oncology Network (IPPON), University of Antwerp, Antwerp, Belgium

[3]Research in Dosimetric Applications (RDA), SCK CEN, Mol, Antwerp, Belgium

[4]NuTeC, CMK, Hasselt University, Hasselt, Belgium

Correspondence
Michaël Claessens, Department of Radiation Oncology, Iridium Netwerk, Oosterveldlaan 24, Antwerp, Belgium.
Email: michael.claessens@zas.be

Funding information
Flemish League Against Cancer, Belgium, Grant/Award Number: 000019356

Abstract

Background: Plane-parallel ionization chambers are the recommended secondary standard systems for clinical reference dosimetry of electrons. Dosimetry in high dose rate and dose-per-pulse (DPP) is challenging as ionization chambers are subject to ion recombination, especially when dose rate and/or DPP is increased beyond the range of conventional radiotherapy. The lack of universally accepted models for correction of ion recombination in UDHR is still an issue as it is, especially in FLASH-RT research, which is crucial in order to be able to accurately measure the dose for a wide range of dose rates and DPPs.

Purpose: The objective of this study was to show the feasibility of developing an Artificial Intelligence model to predict the ion-recombination factor—k_{sat} for a plane-parallel Advanced Markus ionization chamber for conventional and ultra-high dose rate electron beams based on machine parameters. In addition, the predicted k_{sat} of the AI model was compared with the current applied analytical models for this correction factor.

Methods: A total number of 425 measurements was collected with a balanced variety in machine parameter settings. The specific k_{sat} values were determined by dividing the output of the reference dosimeter (optically stimulated luminescence [OSL]) by the output of the AM chamber. Subsequently, a XGBoost regression model was trained, which used the different machine parameters as input features and the corresponding k_{sat} value as output. The prediction accuracy of this regression model was characterized by R^2-coefficient of determination, mean absolute error and root mean squared error. In addition, the model was compared with the Two-Voltage (TVA) method and empirical Petersson model for 19 different dose-per-pulse values ranging from conventional to UDHR regimes. The Akiake Information criterion (AIC) was calculated for the three different models.

Results: The XGBoost regression model reached a R^2-score of 0.94 on the independent test set with a MAE of 0.067 and RMSE of 0.106. For the additional 19 random data points, the k_{sat} values predicted by the XGBoost model showed

Abbreviations: 2D, two dimensional; AI, artificial intelligence; DPP, dose-per-pulse; DR, dose rate; Gy, gray; MeV, mega-electron volt; MAEmean absolute error, mean absolute error; ML, machine learning; RMSE, root mean squared error; OSLoptically stimulated luminescence, optically stimulated luminescence; PFR, pulse frequency rate; TVA, two-voltage analysis; UHDRultra high dose rate, ultra high dose rate.

Michaël Claessens and Verdi Vanreusel contributed equally to this work.

to be in agreement, within the uncertainties, with the ones determined by the Petersson model and better than the TVA method for doses per pulse >3.5 Gy with a maximum deviation from the ground truth of 14.2%, 16.7%, and −36.0%, respectively, for DPP >4 Gy.

Conclusion: The proposed method of using AI for k_{sat} determination displays efficiency. For the investigated DPPs, the k_{sat} values obtained with the XGBoost model were in concurrence with the ones obtained with the current available analytical models within the boundaries of uncertainty, certainly for the DPP characterizing UDHR. But the overall performance of the AI model, taking the number of free parameters into account, lacked efficiency. Future research should optimize the determination of the experimental k_{sat}, and investigate the determination the k_{sat} for DPPs higher than the ones investigated in this study, while also evaluating the prediction of the proposed XGBoost model for UDHR machines of different centers.

KEYWORDS
dosimetry, FLASH, machine learning, radiation therapy, UHDR, XGBoost model

1 | BACKGROUND

The main goal of radiation therapy (RT) is to treat cancer patients with minimal adverse effects caused by radiation damage to the surrounding healthy tissue. In RT, normal tissue toxicity is the limiting factor of the therapy. In the past decades, several improvements have been introduced to reduce the dose delivered to the normal tissue. However, most of these improvements are based on the ballistics of the beam and the possible gains from further improvements on this aspect are marginal.[1] Recently, a novel technique, named FLASH-RT, proved to significantly increase the efficiency of RT, as it is based on the inherent radiation response of the tissues. This modality uses ultra-high dose rates (UHDRs), which have shown to strongly reduce normal tissue toxicity with the preservation of the anti-tumor response in pre-clinical experiments.[2] Moreover, the use of UHDRs comes with practical benefits, such as minimized intra-fractional motion and increased patient comfort.[3] All this can establish FLASH-RT as a revolutionary treatment modality.

However, one of the main challenges that needs to be addressed to successfully translate FLASH studies into the clinical stage, is the development of robust and accurate dosimetry protocols.[4] For dosimetry and the monitoring of clinical electron beams, plane parallel ionization chambers are to date the golden standard.[5] The absorbed dose to water can then be calculated according to established international protocols like the International Atomic Energy Agency Technical Reports Series 398 (IAEA TRS 398) or American Association of Physicists in Medicine TG 51 (AAPM TG 51).[6,7] The reading of the ionization chamber needs correction for several effects. One of them is ion-recombination occurring inside the chamber.[5,8] This correction strongly depends on the dose-per-pulse (DPP), therefore it is small for electron beams used in conventional RT (i.e., DPP < 1.3 mGy), but becomes more relevant in intra-operative RT (i.e., DPP < 130 mGy), and extremely important in FLASH-RT (i.e., DPP in the range of 0.5–10 Gy), where corrections >60% are needed.[3,9]

Different models have already been developed to describe the ion recombination in the ionization chamber: 1) the three general Boag equations and Boag-derived Two Voltage Analysis (TVA) method, for conventional RT, 2) the Di Martino models, developed for IOeRT, and 3) the empirical Petersson logistic model focusing on UHDR RT.[3,5,10] However, none of these models can accurately estimate the ion-recombination correction factor (k_{sat}) for a wide range of DPPs.[9] The lack of universally accepted models for UDHR is still an issue as it is, especially in FLASH-RT research, to accurately measure the dose for a wide range of dose rates and DPPs.[9,11]

To address this issue, we aimed to develop an user-friendly artificial intelligence (AI) model to directly predict the k_{sat} correction factor based on different machine parameters. A XGBoost regression model was used. This is a more efficient version of gradient boosting that attempts to accurately predict a target variable by combining the estimates of a set of simpler, weaker models. XGBoost minimizes a regularized (L1 and L2) objective function that combines a convex loss function (based on the difference between the target and the predicted outputs) and a penalty term for model complexity.[12] In this study, the ion-recombination correction factor k_{sat} was predicted for a plane parallel Advanced Markus (AM) chamber. In addition, the predicted k_{sat} of the AI model was compared with the currently applied analytical models. It should be stated that the concept of the proposed methodology relies strongly on the robustness of the reference dosimetry system. As the latter is still a topic of research, the proposed method in this paper

should be considered as a proof-of-concept, using OSL and alanine for reference dosimetry.[11] Other dosimetry systems can be applied or explored in the future.

2 | METHODS

2.1 | Experimental determination of the ion-recombination correction factor (k_{sat})

The absorbed dose to water measured by the ionization chamber can be calculated according to international protocols (e.g., IAEA TRS-398)[6] using to the following equation:

$$D = M \cdot N'_{^{60}Co,Dw} \cdot k_{Q_0Q'} \cdot k_h \cdot k_{T,p} \cdot k_{el} \cdot k_p \cdot \boldsymbol{k_{sat}} \quad (1)$$

where M is the measured charge, $N'_{Co\text{-}60,Dw}$ is the calibration coefficient of the ionization chamber for absorbed dose to water in a ^{60}Co beam, $k_{Q0Q'}$ is the beam quality correction factor, k_h is the humidity correction factor, $k_{T,P}$ is the air density correction factor, k_{el} is the calibration factor of the used electrometer, k_p is the factor to correct for the polarizing voltage effect, and k_{sat} is the ion-recombination factor which accounts for incomplete charge collection due to recombination effects inside the chamber. In this study, we use an Advanced Markus plane parallel ionization chamber (*PTW, Freiburg, Germany*). For the geometric and electrical details of the used AM chamber, we refer to Table S1.

The ion-recombination correction factor (k_{sat}) was experimentally determined via the following formula:

$$\boldsymbol{k_{sat}} = \frac{D_{ref}}{M \cdot N'_{^{60}Co,Dw} \cdot k_{Q_0Q'} \cdot k_h \cdot k_{T,p} \cdot k_{el} \cdot k_p} \quad (2)$$

where D_{ref} corresponds to the dose measured by the reference dosimeter. The reference dosimeter should be dose rate and DPP independent in the range of the measurements.

2.2 | Reference dosimetry in UHDR

As no standardized procedures and dosimeters yet exist for UHDR dosimetry, the optically stimulated luminescence (OSL) system, developed by Agfa N.V. (*Mortsel, Belgium*), was used. The OSL system consists of a BaFBr solid state OSL screen (Table S2), that is read out using a computed radiography scanner (CR-15).[13–15] The time between the start of the irradiation and readout was kept constant at 1 min 17 s to account for dark decay.[16] The first of this system in UHDR show no dose rate dependence.[17–19] In addition, for a subset of data points, the OSL system was benchmarked using alanine electron paramagnetic resonance (EPR) dosimetry (*NuTec, Hasselt, Belgium*). Based on this comparison, a trend line was constructed to scale the OSL dose response. Alanine pellets are considered dose rate independent and are frequently used for UHDR dosimetry.[11,20] For a comparison in characteristics between these detectors, we refer to Table S3.

TABLE 1 An overall representation of the different machine parameters, which were used as input data for the ML model.

Parameters	Settings
Modality	Conventional; UHDR
Nominal beam energy (MeV)	7; 9
Pulse repetition frequency (Hz)	100; 200
Pulse length (μs)	0.5 - 1 - 1.5 - 2 - 2.5 - 2.7 - 3 - 3.2 - 3.5 - 4
Source surface distance (cm)	78.1 - 91.9 - 103.35 - 114.85 - 126.3 - 137.85 - 149.4 - 160.8 - 172.2 - 183.8

2.3 | Measurements

In Table 1, the machine parameters used in this study are listed. All measurements were performed using the ElectronFlash (EF, *SIT Sordina, Aprilia, Italy*), which is a dedicated research accelerator for FLASH-RT. This system is designed to generate electron beams with a broad window of DR and DPP, both in conventional and UHDR. The pulse length could only be altered in UHDR (from 0.5 to 4 μs), and was fixed to 1 μs in conventional modality. The k_{sat} was determined for the various combinations of settings reported in Table 1. These machine settings were used as input features for the AI model. As a result, a total number of 425 measurement was collected with a variety in machine parameter settings. The distribution of the k_{sat} values in function of the different settings can be found in Figure 1.

The experimental setup is shown in Figure 2. The grey tapes at the side of the table correspond to the different SSD positions, which were defined to vary the pulse amplitude, and thus DPP. The AM chamber was placed in a solid water phantom (RW3) with 15 mm build-up and at least 50 mm backscatter. This way, the effective point of measurement of the AM is centered in the plateau of maximal dose deposition in the depth deposition dose curve. The OSL sheet was put in front of—and in contact with the AM chamber to allow simultaneous irradiation.

2.4 | Machine learning-based regression model

A ML-based XGBoost regression model was trained in a supervised way to predict the k_{sat} factor directly.[21]

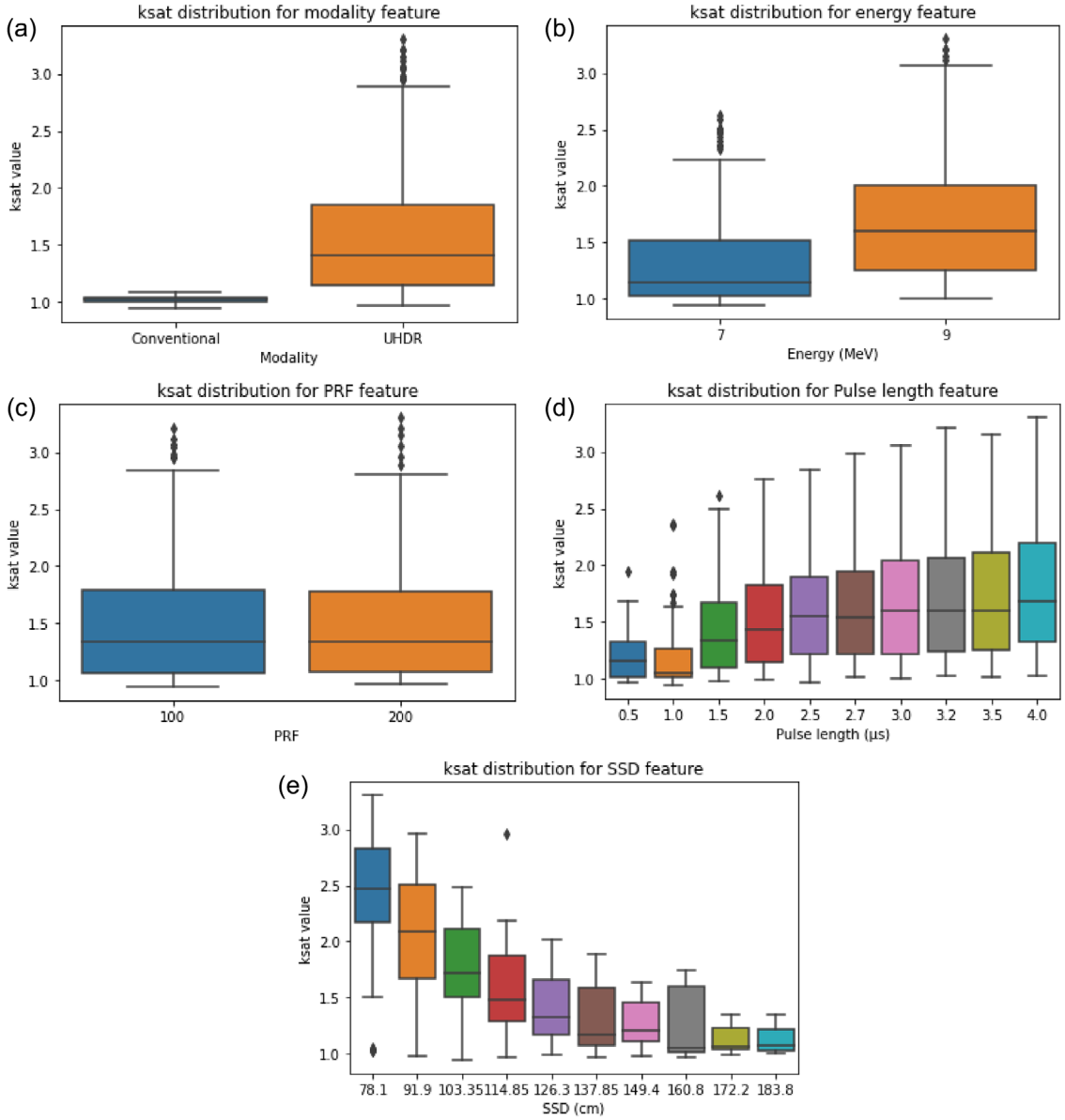

FIGURE 1 Boxplots that show the distribution of the k_{sat} values in function of (a) modality, (b) energy, (c) PRF, (d) pulse length, and (e) SSD.

XGBoost is a form of ensemble learning, which combines individual models (i.e., base learners) to get a single prediction.[12] All input features that were used to train the ML model are represented in Table 1. As corresponding output, the experimentally obtained k_{sat} factor was used (Equation (2)). The original dataset of 425 measurements was divided into a training and test set with a standard ratio of 80/20. During the training phase, various hyperparameter combinations such as number of estimators, maximum depth, regularization term (i.e., L1/L2 regularization on leaf weights), learning rate, etc. were exhausted by grid search after k-fold cross-validation ($k = 5$). Afterwards, the performance of the overall best model was checked on the independent test set by the mean absolute error (MAE), root mean squared error (RMSE), and R-squared (R^2-coefficient of determination) with additionally prediction error and residuals plots. Scripting was done in Python using dedicated ML libraries (i.e., TensorFlow/scikit-learn).

2.5 | Model validation against analytical models

In order to test whether the AI model can overcome certain limitations of the current applied analytical formulas, the k_{sat} predictions from different models were compared with the experimentally measured for 19 randomly selected data points. Note that these points were neither in the training nor test set of the AI model.

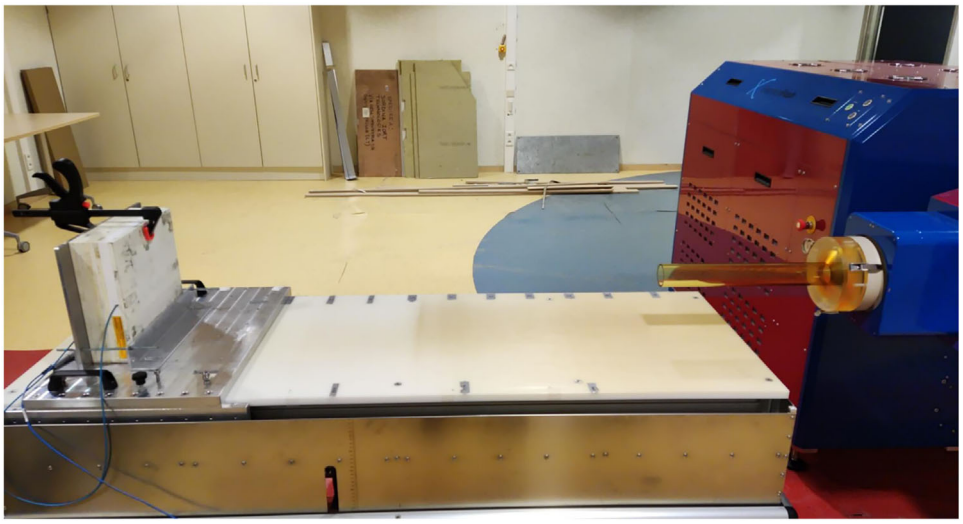

FIGURE 2 An overall representation of the experimental setup. In this scenario, the phantom is positioned on a SSD of 183.8 cm.

For comparison with the model's output, the k_{sat} value was first calculated by the Boag-derived TVA method (3):

$$\boldsymbol{k_{sat}} = \mathrm{a0} + \mathrm{a1} \cdot \left(\frac{M1}{M2}\right) + \mathrm{a2} \cdot \left(\frac{M1}{M2}\right)^2 \quad (3)$$

where a_0, a_1, and a_2 are constants defined by the voltage ratios (in our case, $a_0 = 1.198$, $a_1 = -0.875$, and $a_2 = 0.677$) and M1 and M2 are the measured collected charges at polarizing voltages of 300 and 100 V, respectively.

Second, the k_{sat} value was calculated according to Petersson empirical model formula[3] (5):

$$\boldsymbol{k_{sat}} = \left(1 + \left(\frac{\mathrm{DPP}\,[mGy]}{U\,[V]}\right)^{\alpha}\right)^{\beta} \quad (4)$$

where DPP is the dose-per-pulse, U is the polarizing voltage across the ionization chamber, and α and β are fitting constants with no physical meaning (with values of 2.5 and 0.144 respectively).

Our model was compared with the two above using the Akaike Information Criterion (AIC) calculated on the independent test set of 20 additional data points. AIC determines the relative information value of the model using the maximum likelihood estimate (i.e., how well the model reproduces the data) and the number of parameters (independent variables) in the model. As the considered sample size was beneath the number of 40, a corrected AIC (AICc) was calculated. The model with the lowest AIC offers the best fit. Moreover, the ΔAIC was determined, that is the relative difference between the best model (which has a ΔAIC of zero) and each other model in the set.

3 | RESULTS

3.1 | Determination of D_{ref} using OSL/alanine

For a subset of data points, the relationship between the measured dose by the OSL system and the alanine dosimeter is shown in Figure 3a. These data points have a linear component that can be described by a best-fit line with equation: $y = 1.0571\ (\pm\ 0.075)\ x - 0.3858\ (\pm\ 0.674)$. This means that the OSL dose is 5.7% lower than the alanine dose, with an error in one of both systems represented by x, where the latter can be determined by the standard error of the y-estimate. In Figure 3b, the residual plot is given to show no bias is present.

3.2 | In-house prediction accuracy

The performance of the overall best model after 5-fold cross validation was validated on an independent test set. The values of the statistical measurements are listed in Table 2. The R^2 value for the model is 0.94, which means that 94% of the variability observed in the k_{sat} values is explained by the model. The MAE has a value of 0.061, which characterizes the alteration among the original and predictable values. The RMSE has a value of 0.108, which in addition to MAE, implements a quadratic scoring rule that also measures the average magnitude of the error. In Figure 4a, the prediction error plot is shown, where most of the data points are on a straight line (i.e., black dotted). In Figure 4b, the residuals plot is presented, where distributions on the right side indicate that the residuals (actual values-predicted values) are approximately normally distributed.

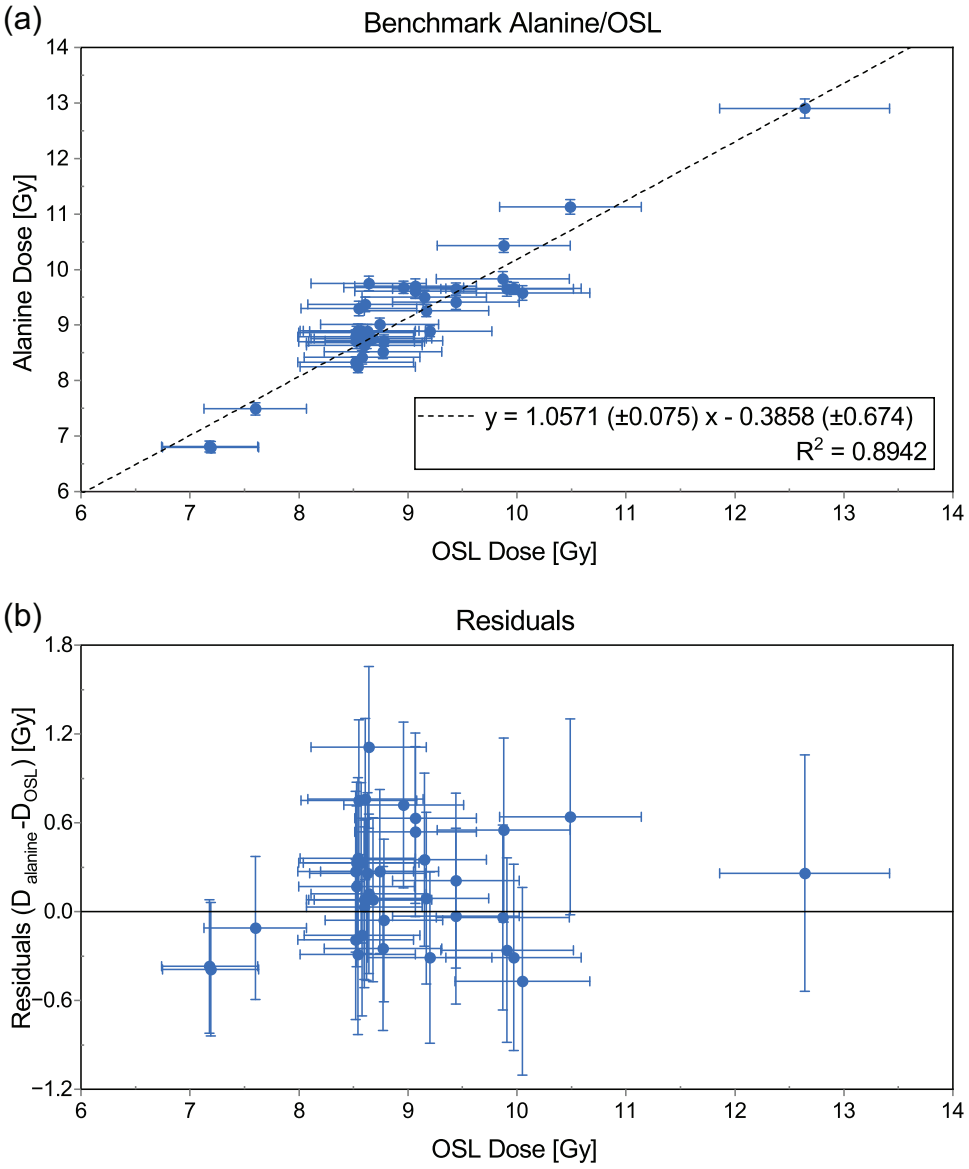

FIGURE 3 (a) Linear regression scatter plot with dashed trend line ($y = 1.0571\ (\pm\ 0.075) \cdot x - 0.3858\ (\pm\ 0.674)$; $R^2 = 0.8942$) relating alanine dose read-out to OSL dose read-out. (b) Residual plot with individual data points as fitted value.

TABLE 2 Results of the statistical measures of the overall ML model on the independent test set.

Statistical metric	Specific value
R^2 value	0.940
MAE	0.067
RMSE	0.108

3.3 | Analytical model validation

For 19 unseen data points evenly spread over the set of machine parameters, which cover the entire range of DPPs typical for conventional and UDHR regimes, the DPP measured with the AM is plotted against the simultaneously measured reference DPP in Figure 5. The AM DPP was corrected for ion recombination by using 1) the TVA method, 2) the empirical Petersson model, and 3) the XGBoost model. The dashed line represents the perfect correction of AM DPP to the reference dosimeter.

For the lower DPP range (0–2 Gy), the k_{sat} corrected DPP was determined with an accuracy better than 36% for all models. For DPPs higher than 2 Gy, the TVA method systematically over- or underestimates the recombination factor, reaching a difference of 18.8% and −13.8% at dose 2.30 and 2.60 Gy, respectively. This difference increases with higher DPPs, with a dose difference of −5.8% at 4.08 Gy, −36.0% at 4.31 Gy, and −25.2% at 4.43 Gy). In contrast, the Petersson and XGBoost models show high agreement for most data points with a DPP lower than 4 Gy, with a

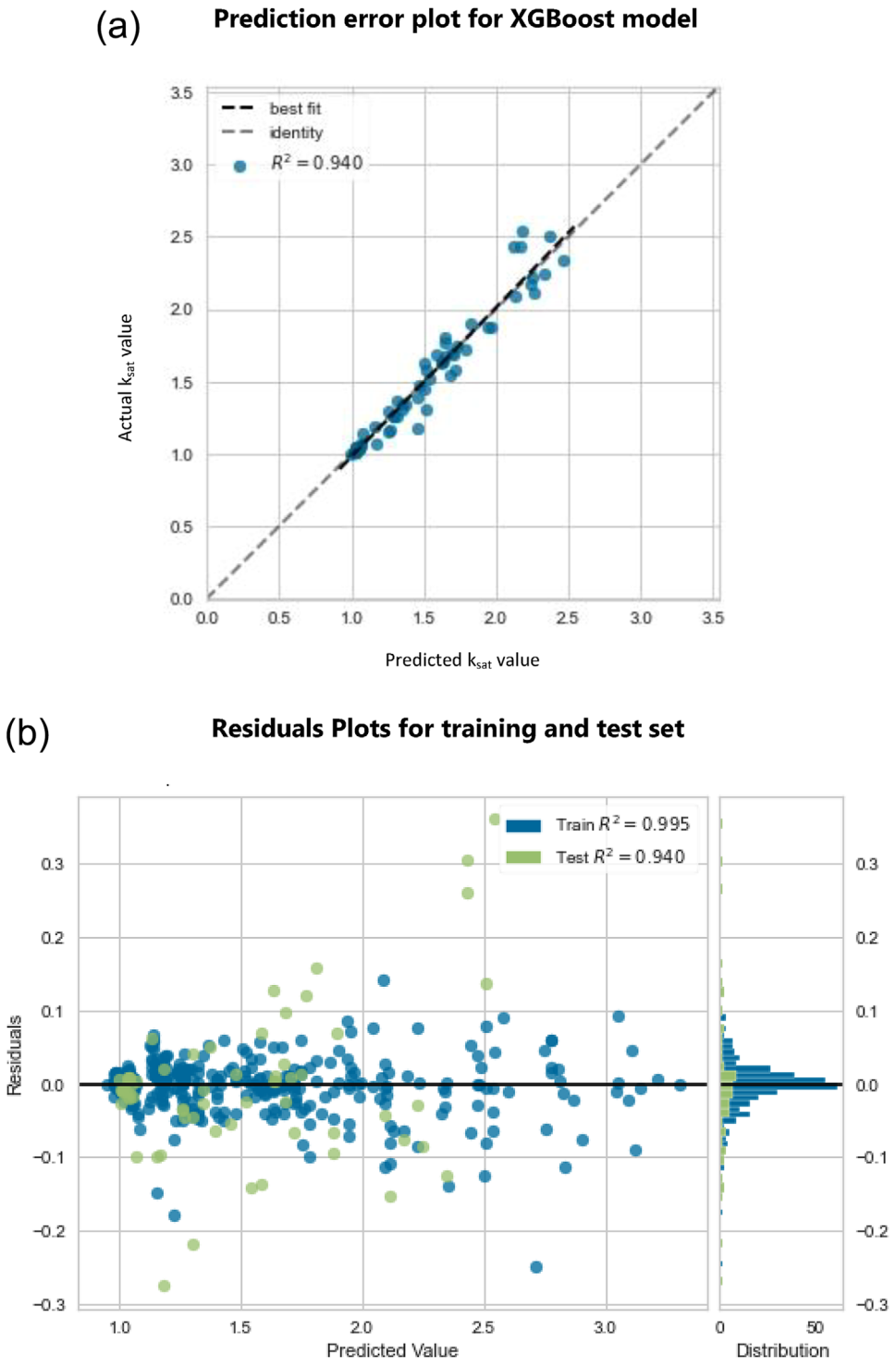

FIGURE 4 (a) The prediction error plot for the XGBOOST model on the independent test set with y the actual value and $\hat{y}$ the predicted value. (b) The residual plots for training and test set.

difference of 15.91% and 3.1% for the Petersson model and 15.1% and 19.1% for the XGBoost model for a DPP of 2.30 and 2.60 Gy, respectively. For data points with DPPs above 4 Gy, the XGBoost model shows differences of 14.2%, −0.85%, and 8.26% from the experimental k_{sat} in comparison to 16.7%, −7.4%, and −1.0% for the Petersson model at 4.08, 4.31, and 4.43 Gy respectively. However, the data points of both models are within the boundaries of prediction uncertainty.

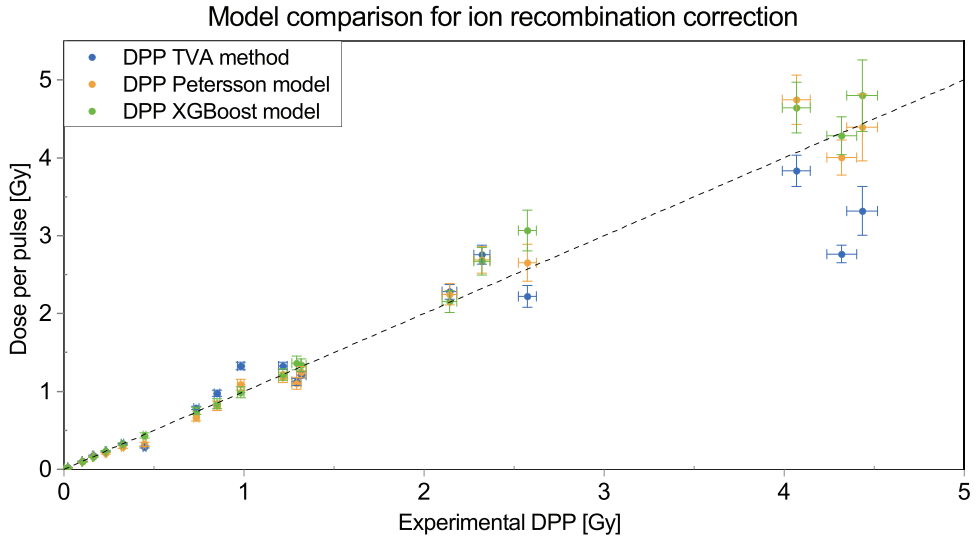

FIGURE 5 Comparison between the DPP measured by the OSL and the AM, where the value of the latter was corrected for ion recombination by means of the k_{sat} factor. This correction was determined by the TVA method (blue), the Petersson empirical model (orange), and the XGBoost regression model (green). The dotted line represents the golden truth, meaning the perfect correction of the ion recombination.

In addition, the AICc is calculated for the three different models.

4 | DISCUSSION

The dosimetric characterization of UHDR electron beams should ideally be performed by DPP and dose rate-independent dosimeters, such as a Fricke-type dosimeter, alanine EPR, and radiochromic film.[11] The clinical utility of such devices is rather limited due to low sensitivity, cumbersome calibration, or long post-irradiation reading time. The absorbed dose can be directly measured with a parallel-plate ionization chamber, which is considered the golden standard for electron dosimetry. One major limitation is that its response should be corrected for the lack of complete charge collection due to ion recombination by means of k_{sat}. Current theoretical models are not capable to predict this correction factor for DPPs typical for FLASH-RT, where high recombination losses (>60%) can occur.[9] In this paper, the feasibility of using an automated method for k_{sat} determination for a parallel-plate ionization chamber is checked, as well as its applicability in high DPP electron beams.

The OSL system was used as a reference dosimeter to determine the experimental k_{sat} value of the ionization chamber for a certain setup. However, as the dose rate response in UHDR beams is still not fully explored, the OSL dose was compared to alanine EPR and scaled when and if needed. Alanine has been proven to be effective for instantaneous dose rates up to about 10^{10} Gy/s and mean dose rates greater than 1 kGy/s, making them a reliable reference dosimeter for UHDR FLASH studies. The benchmark set-up showed a 5.7% lower dose read-out for OSL in comparison to alanine.[11] This study was conducted as a proof-of-concept with OSL as it was available. In future work, it is advised to use better optimized dosimetry systems with better uncertainty for reference in combination with the reported methodology in this paper.

Based on the results of statistical measurements (i.e., Table 2) and prediction error plot on the independent test set, the model has shown to predict k_{sat} values accurately for unseen combinations of machine and setup parameters. To validate the model in comparison to the current available models for k_{sat} calculation, k_{sat} was determined for 19 random data points, evenly spread over the DPP range covered in this study using the different models. These were used to correct the DPP measurement of the AM, which was compared with the experimental DPP in Figure 5. For DPPs typical for UHDR, the approximations used to derive the TVA method are no longer valid and result in an underestimation of the k_{sat} value. This has already been demonstrated before in different studies[3,22] and was validated here, showing the need for alternative methods. The logistic model, proposed by Petersson et al.,[3] provided an accurate prediction across the study-specific full DPP range. The XGBoost model showed high overlap with this model, with all data points falling in each other's uncertainties. For a DPP of 4.08, 4.31, and 4.43 Gy respectively, the XGBoost showed a difference of 14.2%, −0.85%, and 8.26% from the experimental DPP in comparison to 16.7%, −7.4%, and −1.0% for the Petersson model. Based on these results, the k_{sat} values determined by the AI- and Petersson models can be considered equivalent.

TABLE 3 An overview of the AIcc and Delta AICc for every used model to predict the k_{sat} value for the 20 independent data points.

	K	AICc	ΔAICc
XGBoost model	5	21.14	11.42
TVA method	1	9.72	0
Petersson model	2	11.40	1.68

Note: *K* is defined as the number of free parameters.

The AICc comparison between the models (i.e., Table 3), suggests the TVA method is the best performing model, taking the model's complexity into account. However, this model underestimates the required correction for high DPP (>2.5 Gy), as previously discussed. We attribute the superiority of this model to the limited number of validation points, especially at high DPP. Taking both the goodness of fit and the AICc into account, the Petersson model is the superior model, because less parameters are needed to determine the k_{sat} value with similar accuracy as the XGBoost model.

In practice, however, the Petersson model requires prior knowledge of the DPP for every beam parameter setting. Therefore, a high number of measurements are needed to map the entire beam parameter space, especially for highly flexible UHDR beams. We showed the feasibility of the proposed strategy to use an AI model for the determination of k_{sat} as an alternative. This method strongly reduces the number of these time-consuming measurements, since the model is trained on a subsection of the beam parameter space and is yet able to predict the k_{sat} value for every arbitrary beam parameter setup. An additional benefit is that this method is not limited by approximations, as is the case for most analytical models, making it relevant for a wide range of dose rates and DPP. In this regard, the proposed approach could ease the validation of future analytical models by reducing the number k_{sat} values to be experimentally determined.

It should be stated that this study has some limitations. The main limitation is the reference dosimetry, performed with experimental OSL dosimetry sheets. This resulted in large uncertainties and a discrepancy of 5.7% with the more trustworthy alanine dosimetry. Therefore, experimental k_{sat} values smaller than 1 were observed for a subset of data points obtained in the 7 MeV conventional modality. Further investigation is needed to determine the impact on the model. The effect of the sub-optimal reference dosimetry does however not only affect the AI based method, but also the Petersson model, as this relies on the experimental DPP. Therefore, the observed equivalence of the XGBoost model for the k_{sat} value determination is expected to remain valid when the reference dosimetry is optimized. Also, in order to cover the entire sensitive volume of the AM, a 50 mm applicator was needed for this study, limiting the output DPP to 4.5 Gy. Another limitation is the absence of validation for a different UHDR electron machine and configuration. Future studies should investigate the subset of the beam parameters to minimize the required measurements while maximizing the model's performance over a wide range of parameter settings. Also, it should be investigated which beam parameters are relevant, in order to prevent overfitting. In addition, future studies should focus on creating a generic framework for different beam structures and particles.

5 | CONCLUSIONS

It was demonstrated that an AI approach can be used to determine the ion recombination in electron beams. The k_{sat} values determined by the presented AI model were comparable with the ones obtained with the generally accepted alternative methods for k_{sat} determination, including at high dose per pulse. The overall performance of this AI model, taking into account the number of parameters, was inferior compared to these alternatives. It has however the benefit of not requiring measurements for every possible beam parameter setting, which is especially important when moving to UHDR treatments where relevant parameters are frequently varied. Despite proving the feasibility of this approach, more accurate reference dosimetry is needed to improve the model's performance and use it to its full potential, resulting in a fair comparison with the more thoroughly studied alternatives and potentially leading to stronger conclusions. Future research, based on cross-referencing various UHDR electron beam systems, aims at validating the model with different beam outputs.

ACKNOWLEDGMENTS

Michaël Claessens has financial support from a grant from the Flemish League Against Cancer, Belgium, ref: 000019356. The PhD research of the Verdi Vanreusel is funded by the young potential grant, awarded by the SCK CEN Academy.

CONFLICT OF INTEREST STATEMENT

The authors declare no conflicts of interest

REFERENCES

1. Baumann M, Krause M, Overgaard J, et al. Radiation oncology in the era of precision medicine. *Nat Rev Cancer*. 2016;16(4):234-249.
2. Friedl AA, Prise KM, Butterworth KT, Montay-Gruel P, Favaudon V. Radiobiology of the FLASH effect. *Med Phys*. 2022;49(3):1993-2013.
3. Petersson K, Jaccard M, Germond JF, et al. High dose-per-pulse electron beam dosimetry—A model to correct for the ion recombination in the advanced Markus ionization chamber. *Med Phys*. 2017;44(3):1157-1167.

4. Bourhis J, Montay-Gruel P, Gonçalves Jorge P, et al. Clinical translation of FLASH radiotherapy: why and how? *Radiother Oncol J Eur Soc Ther Radiol Oncol*. 2019;139:11-17.
5. Di Martino F, Giannelli M, Traino AC, Lazzeri M. Ion recombination correction for very high dose-per-pulse high-energy electron beams. *Med Phys*. 2005;32(7Part1):2204-2210.
6. Andreo P, Huq MS, Westermark M, et al. Protocols for the dosimetry of high-energy photon and electron beams: a comparison of the IAEA TRS-398 and previous international codes of practice. *Phys Med Biol*. 2002;47(17):3033-3053.
7. Huq MS, Andreo P, Song H. Comparison of the IAEA TRS-398 and AAPM TG-51 absorbed dose to water protocols in the dosimetry of high-energy photon and electron beams. *Phys Med Biol*. 2001;46(11):2985-3006.
8. Konradsson E, Ceberg C, Lempart M, et al. Correction for ion recombination in a built-in monitor chamber of a clinical linear accelerator at ultra-high dose rates. *Radiat Res*. 2020;194(6):580-586.
9. McManus M, Romano F, Lee ND, et al. The challenge of ionisation chamber dosimetry in ultra-short pulsed high dose-rate very high energy electron beams. *Sci Rep*. 2020;10(1):9089.
10. Laitano RF, Guerra AS, Pimpinella M, Caporali C, Petrucci A. Charge collection efficiency in ionization chambers exposed to electron beams with high dose per pulse. *Phys Med Biol*. 2006;51(24):6419-6436.
11. Romano F, Bailat C, Jorge PG, Lerch MLF, Darafsheh A. Ultra-high dose rate dosimetry: challenges and opportunities for FLASH radiation therapy. *Med Phys*. 2022;49(7):4912-4932.
12. Chen T, Guestrin C. XGBoost: A Scalable Tree Boosting System. *Proc 22nd ACM SIGKDD Int Conf Knowl Discov Data Min*. 2016.
13. Leblans P, Vandenbroucke D, Willems P. Storage phosphors for medical imaging. *Mater (Basel, Switzerland)*. 2011;4(6):1034-1086.
14. Wouter C, Dirk V, Paul L, Tom D. A reusable OSL-film for 2D radiotherapy dosimetry. *Phys Med Biol*. 2017;62(21):8441-8454.
15. De Roover R, Berghen C, De Meerleer G, Depuydt T, Crijns W. Extended field radiotherapy measurements in a single shot using a BaFBr-based OSL-film. *Phys Med Biol*. 2019;64(16):165007.
16. Caprioli M, Delombaerde L, De Saint-Hubert M, et al. Calibration and time fading characterization of a new optically stimulated luminescence film dosimeter. *Med Phys*. 2023;50(2):1185-1193.
17. Vanreusel V, Gasparini A, Galante F, et al. Optically stimulated luminescence system as an alternative for radiochromic film for 2D reference dosimetry in UHDR electron beams. *Phys Med*. 2023;114:103147.
18. Christensen JB, Togno M, Nesteruk KP, et al. Al(2)O(3):C optically stimulated luminescence dosimeters (OSLDs) for ultra-high dose rate proton dosimetry. *Phys Med Biol*. 2021;66(8).
19. Motta S, Christensen JB, Frei F, Peier P, Yukihara EG. Investigation of TL and OSL detectors in ultra-high dose rate electron beams. *Phys Med Biol*. 2023;68(14).
20. Bourhis J, Sozzi WJ, Jorge PG, et al. Treatment of a first patient with FLASH-radiotherapy. *Radiother Oncol J Eur Soc Ther Radiol Oncol*. 2019;139:18-22.
21. Breiman L. Random forests. *Mach Learn [Internet]*. 2001;45(1):5-32. doi:10.1023/A:1010933404324
22. Kranzer R, Poppinga D, Weidner J, et al. Ion collection efficiency of ionization chambers in ultra-high dose-per-pulse electron beams. *Med Phys*. 2021;48(2):819-830.

SUPPORTING INFORMATION

Additional supporting information can be found online in the Supporting Information section at the end of this article.

How to cite this article: Claessens M, Vanreusel V, Gasparini A, et al. Automated determination of the ion-recombination correction factor (k_{sat}) in ultra-high dose rate electron radiation therapy. *Med Phys*. 2024;1-10. https://doi.org/10.1002/mp.17085